Separation Science and Technology
Publication details, including instructions for authors and subscription information:
http://www.informaworld.com/smpp/title~content=t713708471

Protein Separation and Focusing in a Transient pH Gradient Column

Suk-Won Chun[a]; Jae-Young Bae[ab]; Jong-Duk Kim[a]
[a] DEPARTMENT OF CHEMICAL ENGINEERING AND BIOPROCESS ERC KAIST, TAEJON, KOREA
[b] Yukong Co., Seoul, Korea

To cite this Article Chun, Suk-Won , Bae, Jae-Young and Kim, Jong-Duk(1995) 'Protein Separation and Focusing in a Transient pH Gradient Column', Separation Science and Technology, 30: 10, 2101 — 2125
To link to this Article: DOI: 10.1080/01496399508013896
URL: http://dx.doi.org/10.1080/01496399508013896

SEPARATION SCIENCE AND TECHNOLOGY, 30(10), pp. 2101–2125, 1995

Protein Separation and Focusing in a Transient pH Gradient Column

SUK-WON CHUN, JAE-YOUNG BAE,* and JONG-DUK KIM†
DEPARTMENT OF CHEMICAL ENGINEERING AND BIOPROCESS ERC
KAIST
373-1 KUSONG-DONG, YUSUNG-KU, TAEJON, 305-701, KOREA

ABSTRACT

The simulation of a chromatofocusing column for the separation of a model mixture of four proteins, sperm-whale myoglobin, horse myoglobin, transferrin, and albumin, was performed under transient pH gradients and by computer calculation with a differential model including the buffering action. A simulated mixture of four proteins was eluted at the pH of their isoelectric points, and the internal elution pattern of horse myoglobin was visually determined. The focusing effect of protein by pH was illustrated with the elution of intermittent feeds into a single band. The smooth and linear pH gradients, having interaction with ion exchanger and mixed buffers, were produced by a differential model with a model buffer for the pH gradients and the protein elutions. The calculated linear pH gradients and elution profiles showed good agreements with experiments. The protein separation and focusing effect were calculated with a model buffer and the differential model.

INTRODUCTION

Among the various methods of protein separation, chromatofocusing has been introduced as a distinctive technique combining the high resolving power of isoelectric focusing and the convenience of chromatography (1–3). Following the works of Sluyterman et al. (4–7), the strong focusing effects at the isoelectric points of proteins, generated by the chemically defined internal pH gradient in an ion-exchange column, have been re-

* Current address: Yukong Co., Seoul, Korea.
† To whom correspondence should be addressed.

ported for a number of biologically active fluids (8–14, 16–18, 20). In addition to the focusing effect, there are several advantages: rapid separation, easy operation and column selection, and no cooling problems like those of electrophoresis (8–10).

In this study, experimental and computational simulations were performed in order to investigate protein separation and the focusing effect in a transient pH gradient column. The transient internal pH gradients were generated by flowing an elution buffer through gels maintained at a certain pH, and a model mixture of four proteins was separated. The focusing effect of proteins for sequential feeds was also investigated for preparative purposes.

THEORETICAL CONSIDERATIONS

Surface charges of proteins can be regulated by protons or counterions adsorbed on the surface (20). When the pH is equivalent to the isoelectric point of a protein, the zeta potential falls to zero and the surface charge reaches zero (zero point of charge, called the isoelectric point, pI). In an ion-exchange column packed with an anionic exchanger and operating under the gradient pH, proteins would be concentrated near the pHs of their isoelectric points. Here, the linear gradient of pH will be most appreciated for its good resolution and reproducibility, and therefore the buffers are required to have a constant buffering capacity over a wide pH range (5, 6). In spite of the availability of commercial products, the complex internal mechanisms have not been elucidated to the point of including all of the physical interactions (5, 21).

Transient pH Gradient in the Ion-Exchange Column

The pH variation can be calculated stagewise by mixing a buffer flowing through gels and a stagnant buffer between gels, and by incorporating the buffering action of buffers (4, 7). When equal volumes of aliquots of both phases are mixed, the pH can be determined from the amounts of the moving phase and the stationary phase, and from the buffering capacities. Unfortunately, the internal profile and elution curves of the difference model depends on the mesh size (24).

Differential Model with Buffering Action

Since a column packed with gels consists of the free volume and the stationary phase of gels, the transient material balance of the moving phase can be given with the assumption of no radial dispersion. Let an infinitesimal increment of the axial direction from z to $z + dz$ consist of gels, the

stationary phase, and the moving phase, as shown in Fig. 1. As is the case of an ion-exchange column (21), the transient concentration of proton in the moving phase can be determined from the axial diffusion, the bulk mixing, and the regulation of proton by gel interaction and buffer action. The transient balance of the moving phase can be given by

$$\frac{\partial c}{\partial t} = D_z \frac{\partial^2 c}{\partial z^2} - \nu \frac{\partial c}{\partial z} - \frac{1}{\phi} \frac{\partial n}{\partial t} - F(c_i) \tag{1}$$

where the c and n are the concentrations of proton at the moving phase and the stationary phase, respectively. In Eq. (1), the first term on the right-hand side represents the axial dispersion of proton, the second the bulk convective flow, the third the generation of proton from the stationary phase, and the last the regulation of proton by buffering molecules (appearance and disappearance of proton by binding with buffer molecules). D_z represents the axial diffusion coefficient of proton in the moving phase (but radial diffusivity is neglected), ν is the superficial axial velocity of the eluent, ϕ represents $\epsilon/(1 - \epsilon)\epsilon_s$ for the packing state function, and ϵ and ϵ_s the void volume fractions of the moving and stationary phases, respectively. The proton generation from the stationary phase can be calculated from

$$\partial n/\partial t = k_a(c - n/Ke) \tag{2}$$

where k_a is the mass transfer rate constant multiplied by the transfer area, and Ke is the equilibrium constant of proton binding to gel. The initial values and the boundary values are given by,

$$c = c^0, \; n = Kec^0, \qquad \text{for } z > 0 \text{ and } t = 0 \tag{3}$$

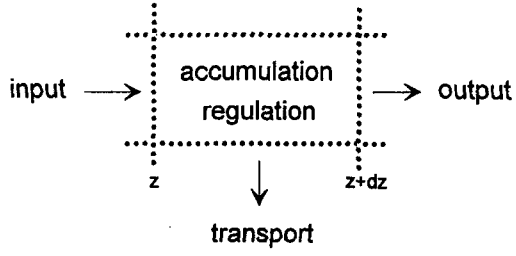

accuml. = input $\big|_z$ - output $\big|_{z+dz}$ - transport into interface - regulation

FIG. 1 Differential model of ion-exchange column with buffers.

$$c = c^{i}, \qquad \text{at } t > 0 \text{ and } z = 0 \tag{4}$$

where c^0 stands for the initial proton concentration of the bed and c^i for the input concentration of the elution buffer. For the moving phase, the mass flux though the boundaries is given by

$$\partial c/\partial z = 0, \qquad \text{for } t > 0 \text{ and } z = \text{infinite} \tag{5}$$

Using the boundary conditions of Eqs. (3), (4), and (5), the differential Eqs. (1) and (2) can be calculated numerically.

Protein Elution

In this transient column the initial pH will be slowly increased and the protons and ions regulated by the polybuffer. Gels and proteins will experience a variation of ionic strength in different pH environments. For protein elutions, the mechanism of an ion exchanger can be approximated by following the adsorption and desorption of proteins. In the differential balance of proteins, however, it is coupled with the amounts of proton by the binding constant, $Ke_{p,i}$, and given by

$$\frac{\partial p_i}{\partial t} = D_{z_{p,i}} \frac{\partial^2 p_i}{\partial z^2} - \nu \frac{\partial p_i}{\partial z} - \frac{1}{\phi} \frac{\partial s_i}{\partial t} \tag{6}$$

$$\partial s_i/\partial t = k_{a_{p,i}}[p_i - s_i/Ke_{p_i}(c)] \tag{7}$$

When the solutions of proteins were injected by pulse, the differential model of Eqs. (6) and (7) (now i represents protein) was solved with the boundary conditions

$$p_i = s_i = 0 \qquad \text{for } z > 0 \text{ and } t = 0 \tag{8}$$

$$p_i = (t - t_s) \qquad \text{at } z = 0 \text{ and } t = t_s \tag{9}$$

$$p_i = \text{finite} \qquad \text{at } z = \text{infinite} \tag{10}$$

The equations for proton and protein (Eqs. 1 and 6), should be calculated simultaneously to simulate the behavior of the protein elution.

Dimensionless Form of Differential Model

For convenience, we consider one component of protein, so we can drop the subscript i. Model Eqs. (1), (2), (6), and (7) were expressed in dimensionless form. The dimensionless groups used are summarized in Table 1.

$$\frac{\partial C}{\partial \tau} = \frac{1}{\text{Pe}} \frac{\partial^2 C}{\partial X^2} - \frac{\partial C}{\partial X} - Pi \frac{\partial N}{\partial \tau} - \alpha_i(C - C_e) \tag{11}$$

TABLE 1
Dimensionless Groups Used in the Model Equations

$C = c/c^0$	$N = n/c^0$	$P = p/p^0$	$S = s/p^0$
$\tau = vt/L$	$X = z/L$	$\mathrm{Pe} = vL/D_z$	$Pi = 1/\phi$
$Po = k_aL/v$	$\mathrm{Pe_p} = vL/D_{z,p}$	$Po_p = k_{a_p}L/v$	

$$\partial N/\partial\tau = Po(C - N/Ke) \tag{12}$$

$$\frac{\partial P}{\partial\tau} = \frac{1}{\mathrm{Pe_p}}\frac{\partial^2 P}{\partial X^2} - \frac{\partial P}{\partial X} - Pi\frac{\partial S}{\partial\tau} \tag{13}$$

$$\partial S/\partial\tau = Po_p(P - S/Ke_p) \tag{14}$$

Initial and boundary conditions were given as follows

I.C.:

$$C = 1,\ N = KeC, \qquad \text{for } \tau = 0,\ X > 0$$
$$P = S = 0 \qquad \text{for } \tau = 0,\ X > 0$$

B.C.: (15)

$$C = C_i \qquad \text{at } \tau > 0,\ X = 0$$
$$C = \text{finite} \qquad \text{for } \tau > 0,\ X = \text{infinite}$$
$$P = \delta(\tau - \tau_s), \qquad \text{at } \tau = s,\ X = 0$$
$$P = \text{finite} \qquad \text{for } \tau > 0,\ X = \text{infinite}$$

Equations (11) and (12) can be simultaneously calculated for proton, resulting in the pH gradient. Using the pH, the binding constant Ke_p can be determined, and then the elution of proteins can be calculated by Eqs. (13) and (14).

Numerical Solution of Differential Model

The basic equations of the moving phase, Eqs. (11) and (13), are parabolic partial differential equations. They are linear as written but become nonlinear when modified to reflect nonlinear equilibrium behavior. The numerical solutions of such equations are usually sought by means of the well-known Crank–Nicholson method (32).

If the diffusion terms in Eqs. (11) and (13) were deleted, they would be hyperbolic rather than parabolic. Parabolic equations such as these are often termed convection dispersion equations because of the presence of both transport modes. When the dispersion term becomes small relative

to the convection term, the solutions take on many of the characteristics of hyperbolic systems, and some difficulties arise in applying the Crank–Nicholson method. Von Rosenberg (27) pointed out that the Crank–Nicholson method is not applicable to hyperbolic equations and has developed the centered-differenced method for the solutions of this form of equations.

In this study the bi-tridiagonal matrix algorithm (27) and the centered-differenced method was applied because our model contains two variable systems.

$$\left.\frac{\partial P}{\partial \tau}\right|_j^{n+1/2} = \frac{1}{\mathrm{Pe_p}}\left.\frac{\partial^2 P}{\partial X^2}\right|_j^{n+1/2} - \left.\frac{\partial P}{\partial X}\right|_j^{n+1/2} - Pi\left.\frac{\partial S}{\partial \tau}\right|_j^{n+1/2} \tag{16}$$

$$\left.\frac{\partial S}{\partial \tau}\right|_j^{n+1/2} = Po_{\mathrm{p}}\left(P_j^{n+1/2} - \frac{S_j^{n+1/2}}{Ke_{\mathrm{p}}}\right) \tag{17}$$

$$\frac{P_j^{n+1}-P_j^n}{\Delta\tau} =$$

$$\frac{1}{2\mathrm{Pe}}\left[\frac{P_{j+1}^n - 2P_j^n + P_{j-1}^n}{(\Delta X)^2} + \frac{P_{j+1}^{n+1} - 2P_j^{n+1} + P_{j-1}^{n+1}}{(\Delta X)^2} + o\{(\Delta t)^2,(\Delta X)^2\}\right] \tag{18}$$

$$-\frac{1}{2}\left[\frac{P_{j+1}^n - P_{j-1}^n}{2\Delta X} + \frac{P_{j+1}^{n+1} - P_{j-1}^{n+1}}{2\Delta X} + o\{(\Delta t)^2,(\Delta X)^2\}\right]$$

$$-Pi\frac{S_j^{n+1}-S_j^n}{\Delta\tau} + o\{(\Delta t)^2\}$$

$$\frac{S_j^{n+1}-S_j^n}{\Delta\tau} + o\{(\Delta t)^2\} = \frac{Po}{2}\left[(P_j^n + P_j^{n+1}) - \left(\frac{S_j^{n+1}+S_j^n}{Ke_{\mathrm{p}}}\right)\right] \tag{19}$$

In the calculation procedure, the values of C_j^{n+1} and N_j^{n+1} are calculated by solving Eqs. (11) and (12). Next, the value of Ke_{p} in Eq. (14) is found from the above values. Finally P_j^{n+1}, and S_j^{n+1} are computed by solving Eqs. (13) and (14).

EXPERIMENTS

Chemicals

Four proteins, horse myoglobin, sperm-whale myoglobin, transferrin, and albumin, and all buffering compounds were purchased from Sigma Chemical Co. and Bio-Rad Laboratories, and used without further purifications. Molecular weights and pIs of proteins are reported in Table 2 (5,

TABLE 2
Molecular Weights and Isoelectric Points (pI's) of Proteins

Protein	Molecular weight	pI	Remark
Albumin	65,000	4.7	(18)
Sperm whale myoglobin	17,800	8.3	Sperm whale (5)
Horse myoglobin	16,600	6.8–7.8	Horse (18)
Transferrin	77,000	5.9	(18)

18, 19). DEAE Bio-Gel A for the ion-exchange column was purchased from Bio-Rad Laboratories, and Polybuffer 74, Polybuffer 96, and ion exchanger PBE 94 from Pharmacia Fine Chemicals (23).

Aqueous solutions of hydrogen chloride (0.1 mole) and sodium hydroxide (1 mole) were formulated with doubly distilled water in our laboratory. The buffering capacities of buffers were determined by titration with hydrogen chloride or sodium hydroxide. Good linearity in the range of experiments was obtained with the acid solution of hydrogen chloride by electric conductivity and pH (20).

Equipment and Methods

The conventional scheme was adapted for the Type C 10/50 chromatographic column of Pharmacia Fine Chemicals and a heavy walled Pyrex tube of outside diameter 12 mm and inside diameter 10 mm. The column was packed with swollen beads of DEAE Bio-Gel A or PBE 94.

After the gels were degassed for 5 to 10 hours, the equilibrium buffer flowed through the gel bed at the rate of 0.3 to 0.8 mL/min. The elution buffer was pumped with a EYELA MicroTube Pump MP-3 (Tokyo Rikakikai Co.) through a silicon tube, and elution aliquots were collected continuously with a fraction collector (Technicon Instrument Co.). When the elution volumes reached 10 to 15 bed volumes and the original pH and electric conductivity were reached, it was assumed that gel was equilibrated with the equilibrium buffer. Then the buffer was eluted through the equilibrated column to produce a linear pH gradient and the protein solutions were injected.

The concentrations of proteins were determined with a Single Path Monitor UV-1 (Pharmacia Fine Chemicals) at 280 nm and recorded with a Gow-Mac Model 70-750 Recorder (Gow-Mac Instrument Co.). The pH was determined with a Dongwoo Medical DP-215 pH meter with a Beckman 39836 Combination Electrode, and the electric conductivity with a YSI Model 31 Conductivity Bridge with a 3404 Cell (Yellow Springs In-

strument Co.). The data were filed in a personal computer. The internal peaks of proteins were determined visually and by taking pictures. The horse myoglobin was a dark brown.

RESULTS AND DISCUSSIONS

Parameters: Model Buffer, Binding Constant, and Mass Transfer Coefficients

Model Buffer

The function $F(c)$ in Eq. (1) requires information about the components of buffer, i.e., Polybuffer 96. However, data are not available, but the linearity of the titration curve of Polybuffer 96 was obtained by the experiments shown in Fig. 2. Further, it is believed that Polybuffer 96 is a mixture of several common buffer solutions or polyelectrolytes. In fact, Hutchens et al. (18, 19) reported the buffer to be a mixture of 31 components. Murel et al. (24, 25) proposed a model in which the buffer capacity varies with the buffer composition. For the mass balance of proton, the concentration of proton in equilibrium solution, $c_{e,i}$, is given by

$$c_{e,i} = c_{0,i} + c_{a,i} - m_i \tag{20}$$

where $c_{0,i}$ is the initial equilibrium concentration, $c_{a,i}$ is the amount of proton added, and m_i is the amount of adsorbed proton due to the buffering capacity as regulated by the buffers. The buffering action $F(c)$ is assumed

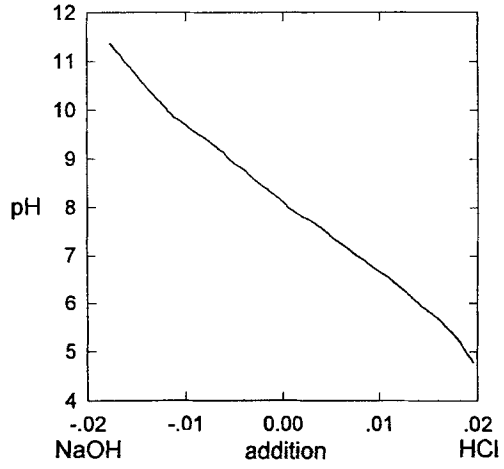

FIG. 2 Titration curve of polybuffer 10% (v/v) Polybuffer 96.

to be a form of the interaction of proton with buffer molecules. The rate function of component i is given by the fractional coverage θ_i ($= m_i/m_{t,i}$) among the available molecules by

$$-dc_i/dt = k_{ad_i}(1 - \theta_i)c_i - k_{d_i}\theta_i \tag{21}$$

where m_t is the total amount of electrolytes covered, and k_{ad} and k_d are the reaction rate constants for the absorption and desorption, respectively.

In the steady state, Eq. (21) can be reduced to

$$\theta_{e,i} = \frac{K_i c_{e,i}}{K_i c_{e,i} + 1} \tag{22}$$

where K_i ($= k_{ad}/k_d$) is the adsorption equilibrium constant. At the elution front, the kinetic equation of proton can be applied with an assumption of local equilibrium because it is nearly saturated at the elution front and can be approximated as $\theta = \theta_e$. Therefore, Eq. (21) becomes

$$-\frac{dc}{dt} = \frac{k_{ad}}{K_i c_e + 1}(c - c_e) = \alpha_i(c - c_e) \tag{23}$$

where α_i contains all the information of constants and the equilibrium concentration of buffer. Further, it is assumed that the elements of a polybuffer are only effective in a certain pH range, namely, near the pI of the element. Below the pH range it is fully saturated, while above this pH it is free of proton. Therefore, the linearized Eq. (23) for a component is limited only within a certain pH range. If the pH deviates from this range, the other components in the polybuffer will respond to the pH changes. Therefore, constant i is a step function within given intervals, ΔpH:

$$\alpha = \sum_{\Delta pH} \alpha_i(\Delta pH) \tag{24}$$

where $\sum$ represents the summation over all pH intervals. In Fig. 2, the pH of the buffer in the titration curve of Polybuffer 96 varies linearly, indicating a wide buffer capacity. As a numerical model, α_i can be deduced from the experiments, as shown in Fig. 3. For our computational purposes, however, the buffer activity coefficient α_i used as a model depending on pH were as shown in Table 3. The set of coefficients provides a linear elution profile of pH.

Mass Transfer Coefficient from Batch Experiments

In batch experiments the amounts of proton that disappear from the bulk phase should be balanced by the amounts transferred into the gel.

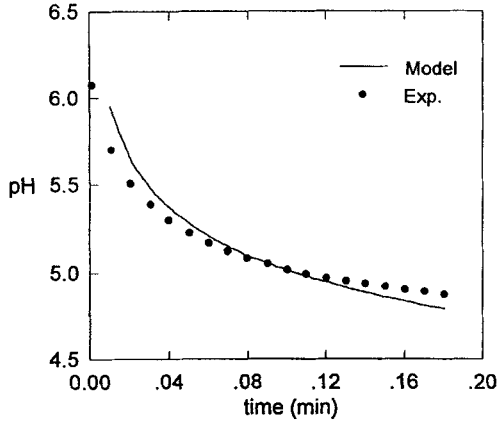

FIG. 3 Buffer action of 10% (v/v) Polybuffer 96 with time. 10% (v/v) Polybuffer 96, 150 mL; 0.1 mol CH_3COOH, 1 mL.

The overall material balance of proton is

$$-\int_0^t V\frac{dc}{dt} = \int_0^t W\frac{dN}{dt}$$

$$V(C_0 - C) = W(N - N_0) \tag{25}$$

TABLE 3
Buffer Activity Coefficients of Model Buffer

pH	α_i	pH	α_i	pH	α_i
9.14	2501	8.96	2450	8.79	2400
8.64	2350	8.50	2300	8.38	2250
8.27	2200	8.16	2150	8.07	2100
7.99	2050	7.92	2000	7.86	1940
7.81	1890	7.76	1840	7.72	1790
7.68	1720	7.65	1670	7.63	1620
7.60	1570	7.58	1520	7.56	1470
7.55	1420	7.53	1370	7.52	1320
7.50	1270	7.48	1220	7.46	1170
7.44	1120	7.41	1070	7.38	1020
7.34	970	7.29	920	7.24	870
7.19	820	7.12	760	7.05	700
6.96	640	6.87	540	6.76	440
6.65	330	6.52	300	6.37	100
6.22	25	6.10	5	6.04	4.5
5.97	2	Below 5.97	1		

where V is the volume of the bulk solution, W is the volume of ion-exchanger, C is the proton concentration in solution, and N is the proton concentration in gel. Suppose that the mass transfer resistance between the bulk solution and the stationary liquid phase in the gel surface is smaller than that between the stationary liquid phase and the gel. Considering only the interface between gels and bulk phases, the transfer rate is given by

$$\frac{dN}{dt} = k_a(C - N/Ke) = -\frac{V}{W}\frac{dC}{dt} \tag{26}$$

Combining Eqs. (2), (6), (25), and (26), the concentration change is given by,

$$\begin{aligned}\frac{dC}{dt} &= -C\left(\frac{k_a}{Ke} + \frac{k_a W}{V}\right) + \frac{k_a}{Ke}\left(C_0 + \frac{WN_0}{V}\right) \\ &= -\sigma C + \pi\end{aligned} \tag{27}$$

where

$$\sigma = \frac{k_a}{Ke} + \frac{k_a W}{V} \tag{28}$$

$$\pi = \frac{k_a}{Ke}\left(C_0 + \frac{WN_0}{V}\right) \tag{29}$$

The initial concentration is represented by the subscript 0, k_a is the mass transfer coefficient, and Ke is the equilibrium constant. Integrating Eq. (27), the concentration of bulk solutions is given by

$$C = \frac{\pi}{\sigma} + D\exp(-\sigma t) \tag{30}$$

where D is the integral constant. From curve fitting of C vs t, we have π and σ, which contain the mass transfer coefficient and the equilibrium constant. The mass transfer coefficient of the proton of PBE 94 was determined from batch experiments, and the constant in the model can be evaluated by using Eq. (30) as in Fig. 4, and k_a was 25 (1/min).

Binding Constants of Proteins Ke_p

In the Sluyterman model a protein molecule will simply shift its position, flowing down the column at the same rate as the eluent if the total charges of the protein molecule and of the ion exchanger have the same sign. If they are of opposite sign (the "all-or-none" model) (2), the protein may not be displaced but adsorbed. For protein elutions, however, there is continuous adsorption and desorption through the ion exchanger. Figure

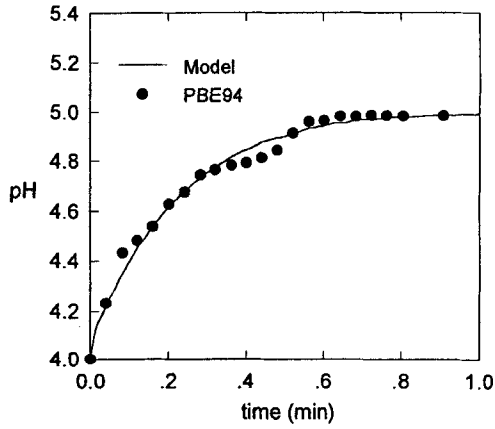

FIG. 4 Buffer action of 10% (v/v) PBE 94 with Time. PBE 94, 50 mL.

5 showed that the binding constant is a strong function of pH. For the calculation of the binding of protein, the constant Ke_p can be approximated by

$$\log Ke_{p,i} = A - B(\mathrm{pI}_i - \mathrm{pH}) \tag{31}$$

where A and B are characteristic constants of protein i.

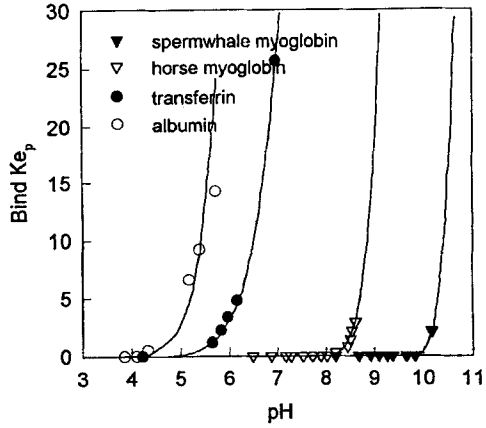

FIG. 5 Binding constants of proteins horse myoglobin, sperm-whale myoglobin, albumin, and transferrin. The lines are the model calculations of Eq. (31).

pH Gradients

The shape of the pH gradient is important in column chromatography for the resolution and separation time. Simulation of the pH gradient was performed experimentally and in model calculations. The buffering action was best performed when the pHs of solutions varied linearly along added amounts of acid or alkaline solutions. In Fig. 6 (PBE 94 and DEAE Bio-Gel A column), smooth and reproducible gradients of pH were achieved in the wide pH range of 9 to 4 when Tris (or ethanolamine) was used as the equilibrium buffer and the Polybuffer as the elution buffer. The concentration of the elution buffer has been reported to increase the pH gradient (5, 16). In our experiments the concentration of equilibrium buffer decreased the gradients, but the effect was smaller than that of the elution buffer. An increase in the flow rate of the medium and in the length of the column reduced the gradient (5, 6).

DEAE Bio-Gel A made a stiffer gradient than did PBE 94 because the buffering capacity of DEAE Bio-Gel A is only one-fifth that of PBE 94, which is consistent with the observations of Sluyterman and Wijdenes (7). Whether protein samples were introduced or not (Fig. 6), the electrical conductivities showed a large irregularity in the early stage of elutions. After one bed volume of elution, a rapid drop was observed which then smoothed out with a minimum in the range of one space time. Here, ions affecting the conductivities of the media may be proton and Cl^-. Since proton combines with a buffer molecule at this pH, the concentration of

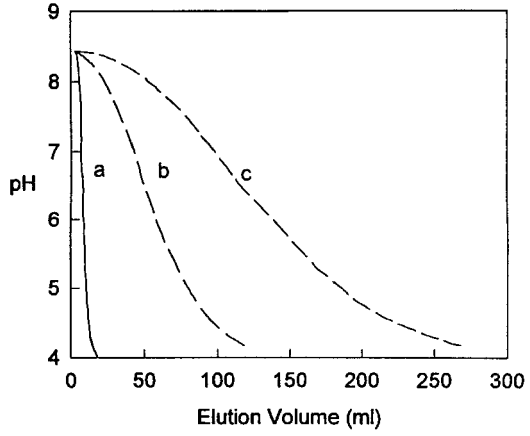

FIG. 6 Buffer capacity of DEAE Bio-Gel A and PBE 94. (a) Water, (b) DEAE Bio-Gel A, (c) PBE 94. Equilibrium buffer, pH 4; elution buffer, pH 8.4.

proton decreases at this pH. Therefore, the proton concentration of 16 mM HCl in the buffer solution is nearly zero, and the active ions affecting the behavior of conductivity curves will be chloride ions.

Simulation of pH Gradients

In Fig. 6 the pH gradients, packed by PBE 94 and DEAE Bio-Gel A, are given. In our model calculations the function $F(c_i)$, representing the buffering actions by a polybuffer, is made of numerous macromolecules differing in their pIs. Initially, the abrupt change of pH gradients is due to the low buffer concentration because of buffer capacity at high pH. In the computer simulation of Fig. 7, the gradient is reproduced in dimensionless time, $\tau = vt/L$, and the internal profiles are given in Fig. 8.

The effects of each parameter in this model are as follows. The dimensionless Peclet number, Pe, is the ratio of the convective flow to the axial dispersive flow. As Pe increases, the pH gradients change abruptly (9, 26), as shown in Fig. 9. As the convective flow decreases, the pH gradient changes slowly.

Pi [$= (1 - \epsilon)\epsilon_s/\epsilon$] represents the void structure of a column and is related to the transportation of proton between the moving phase and the gel. Since $(1 - \epsilon)/\epsilon$ is fixed by the packing method, Pi represents the stationary phase on the gel surface. Figure 10 shows that as Pi increases, the pH gradient and the pH change slowly as expected. Ke represents the partitioning of proton in the moving phase compared to the stationary phase. A large value indicates that the ions are dominant in the stationary

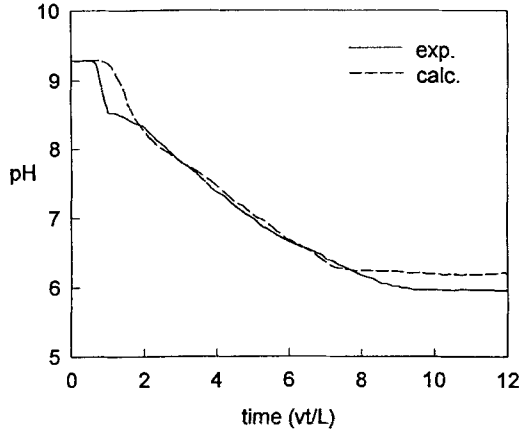

FIG. 7 The pH gradients of PBE94 column with Polybuffer 96 buffer.

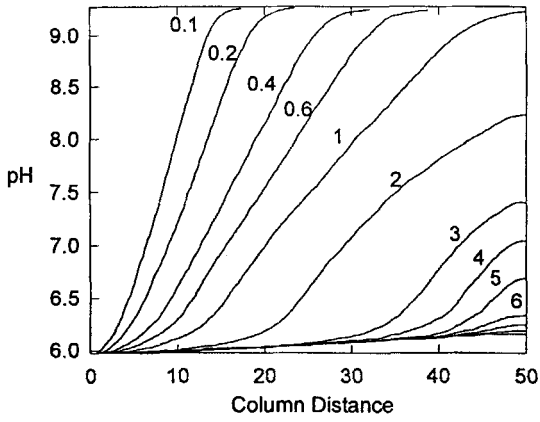

FIG. 8 The internal pH gradient profiles in the column. The numbers represent the dimensionless time.

phase and are slowly eluted, resulting in a curve similar to Fig. 10. The effect of the ratio of the mass transfer to the convective flow is shown in Fig. 11. Below the space time 3.5, as the mass transfer increases, the elution pH increases at small values, but decreases at higher values. If *Po* becomes larger, a smoother pH gradient is achieved after initial drop near one space time.

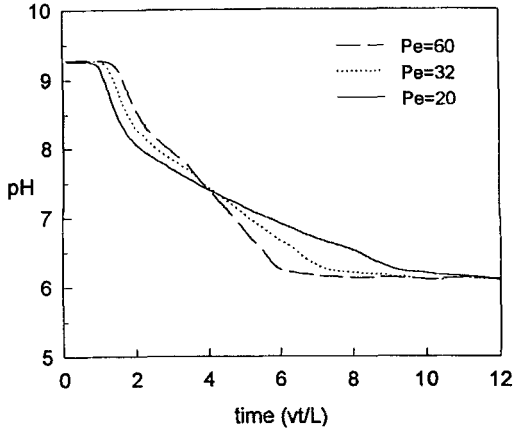

FIG. 9 The effect of Peclet number (Pe = vL/Dz) on the pH gradient (Po = 137.4, Pi = 1.95, Ke = 1.25).

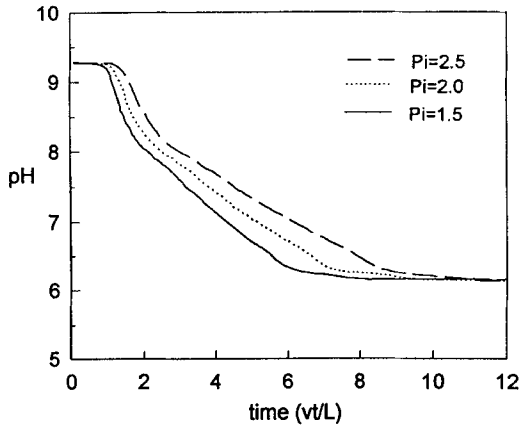

FIG. 10 The effect of the packing state and stationary phase on the pH gradient (Pe = 32.2, Po = 137.4, Ke = 1.25).

In experiments, a linear pH gradient was achieved by the internal method. When the elution was monitored with the residence time (the column length divided by the flow rate), the most significant change of the gradient slope was obtained by a change of the Peclet number and Po. As the axial diffusion and mass transfer to the gel phase increases,

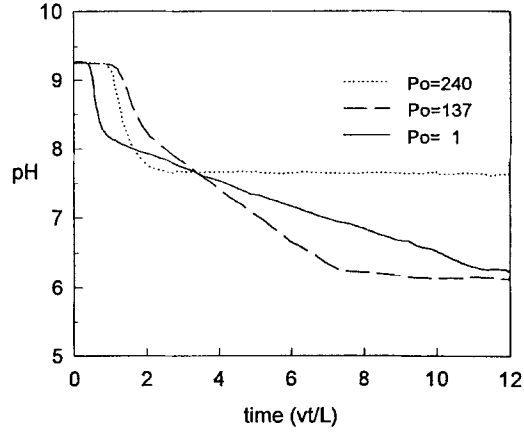

FIG. 11 The effect of mass transfer of gels and convective flow on the pH gradients (Pe = 32.2, Pi = 1.95, Ke = 1.35).

elution reached its equilibrium pH quickly. However, large mass transfer provides a nonlinear profile. If the flow rate increases, Pe increases and *Po* decreases. As a result, the linear gradient zone decreases, and the separation and resolution decrease.

Protein Separation

Protein Elution

An ion exchanger consisting of a crosslinked agarose support is very stable against variations of pH and ionic strength. The gel structure is of the polyethylene-imine type (1). The gel in the column did not change in volume when it was stabilized. The effective liquid volume in the mobile phase was 70 to 80% of the bed volume (25). The individual pI values of the as-purchased proteins were determined and were consistent within 0.25 pH unit (5, 23).

In Fig. 12 the elution profile of horse myoglobin in a column equilibrated to pH 9.27 with 0.025 mole ethanolamine-acetic acid and eluted with Polybuffer 96 equilibrated to pH 5.97 is shown. The filled circles represent the values obtained by taking pictures of myoglobin in the column. The solid line represents the elution profile of the model calculations with interaction, and the dashed line represents the elution profile of the model calculation with no interaction. The buffering action model describes the elution profile of proton and proteins better. Although there were some impurities, the yields of proteins were approximately over 70% (25).

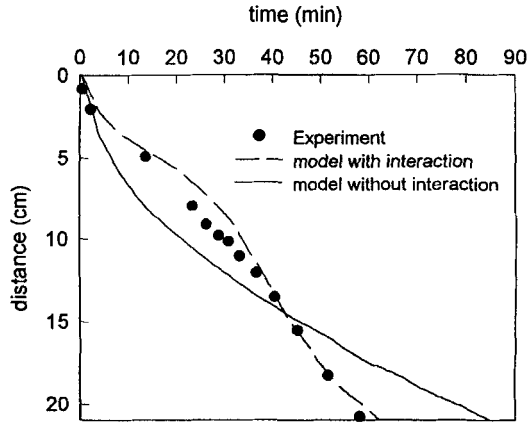

FIG. 12 The elution profile of horse myoglobin. Equilibrium buffer: pH 9.27. Elution buffer: pH 5.97.

Figure 13 shows the elution profile of an artificial mixture of four proteins, horse myoglobin, sperm-whale myoglobin, transferrin, and albumin, with isoelectric points of 8.3, 6.8–7.8, 5.9, and 4.7, respectively. The mixed sample was prepared in 8 mL of equilibration buffer by mixing 4 mg of each protein and the bed volume, 23.6 mL packed with PBE 94 in a C 10/50 column of Pharmacia. The equilibration buffer was 0.025 M ethanolamine-HCl, pH 9.3, and the elution buffer with a rate of 0.6 mL/min was 10% (v/v) PB 74/PB 96 (7:3)-HCl, pH 3.94. One solid line represents the concentration chromatogram for optical density, the other solid line is for the pH of the eluent, and the dashed line is for electric conductivity, mmhos/cm. The vertical arrow indicates the start of 1 M HCl washing.

In order to calculate the pH gradient and the protein elution when the protein solutions are injected by pulse, the differential model of Eq. (1) should be simultaneously solved with the boundary conditions. Further, the buffering action model of $F(c)$ should be used for accurate estimates of the elution profile of proton and proteins.

The Effect of Parameter on Protein Elutions

Figure 14 shows that the effect of Peclet number is minor for protein elution. Since larger Pe leads to a steeper pH gradient, the elution of protein would be rapid. If Po is larger, protein movement speeds up. A

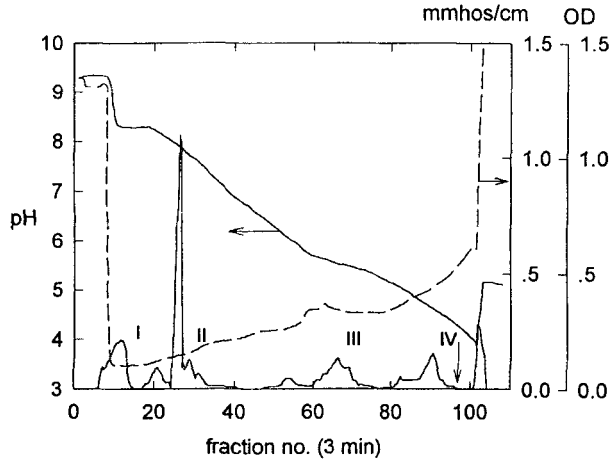

I : spermwhale myoglobin, II : horse myoglobin, III : transferrin, IV : albumin

FIG. 13 The elution profiles of horse myoglobin, sperm-whale myoglobin, transferrin, and albumin with isoelectric points of 8.3, 6.8–7.8, 5.9, and 4.7, respectively.

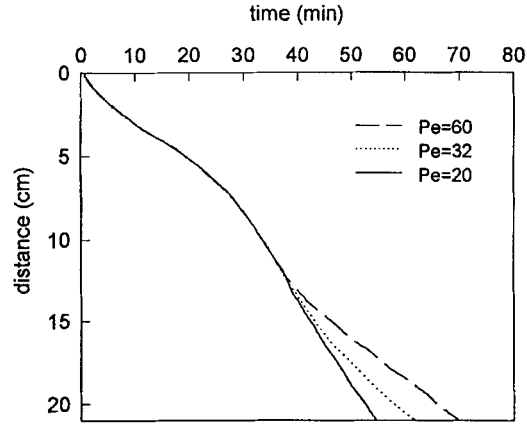

FIG. 14 The effect of Peclet number on the elution of horse myoglobin. Po = 137.4, Pi = 1.95, Ke = 1.25, Pe_p = 16,000, Po_p = 2.76.

large Po increases the adsorption of proton and decreases the interaction of protein with gels. As a result, as Fig. 15 shows, it takes a shorter time for the protein to get out of the column. Pe_p is the ratio of dispersive to convective flow. An increase of dispersion in protein makes the band width broader but has no effect on the position of protein.

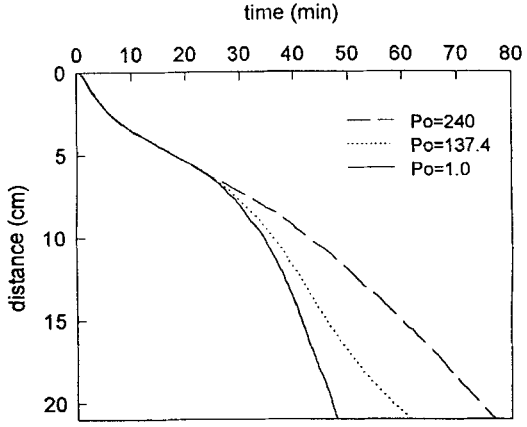

FIG. 15 The effect of Po ($= k_aL/v$) on the elution of horse myoglobin. Pe = 32.2, Pi = 1.95, Ke = 1.25, Pe_p = 16,000, Po_p = 2.76.

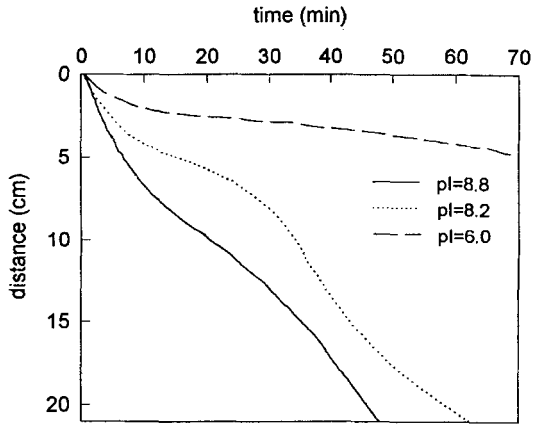

FIG. 16 The elution profiles of mixture of proteins.

Separation in the Mixture of Proteins

Mixture of proteins with pIs of 8.8, 8.2, and 6.0 were eluted (Fig. 16). As the result of simulation, it appears that Pe and *Po* are the most important factors for moving the protein band. In Fig. 17 the effect of *Po* is given for the separation of a mixture of proteins. The interaction of proteins with an ion-exchanger will be small at low *Po*. Therefore, proteins flow almost without separation. Consequently, the flow rate has a critical range in protein separation.

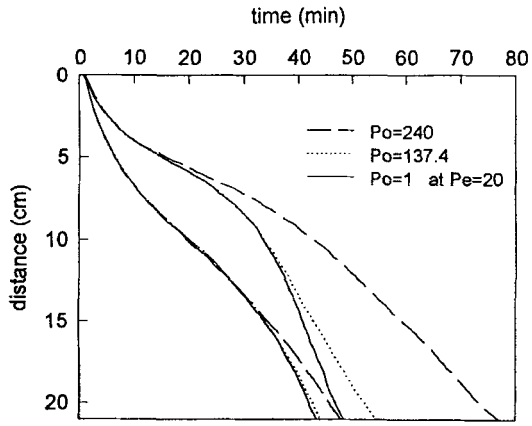

FIG. 17 The effect of *Po* ($= k_a L/v$) on protein separations.

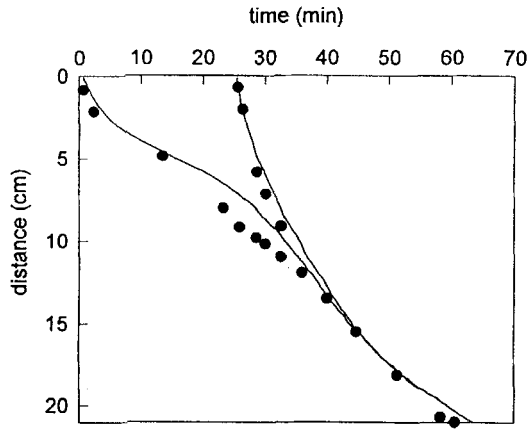

FIG. 18 The focusing effects of myoglobin. The circles represent the experiments and the solid line represents the simulation.

Chromatofocusing Effects

For Fig. 18 the flow profiles of horse myoglobin in the internal column were measured at sequential feeds by taking pictures. The circles represent the results, and the lines represent the elution profile of the model with interaction. After the first sample had flowed down to a certain point, a second sample with the identical protein was injected. As the flow advanced, the main peaks of the solutions merged at the location where the

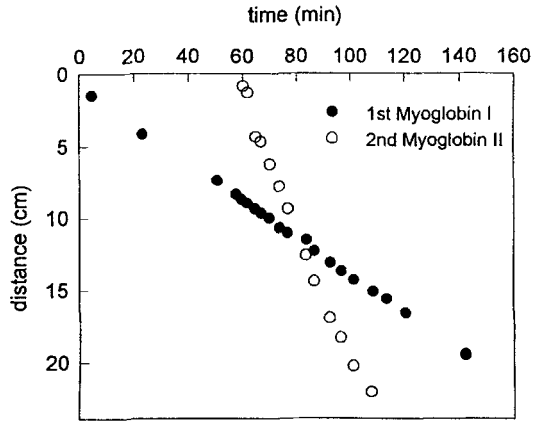

FIG. 19 The elution of horse myoglobin (I) and sperm-whale myoglobin (II).

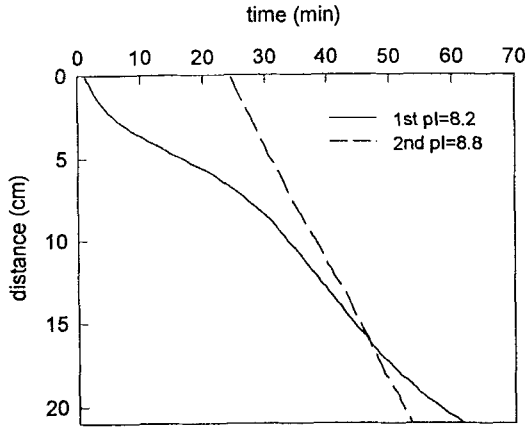

FIG. 20 The simulation of the elution of two proteins with different pIs.

transient pH was equivalent to the pI, and the proteins flow down together until they were eluted. This experiment indicated that protein flows fast when the difference (pH − pI) is negative, and that the protein can be accumulated into a band at the pH until eluted. This phenomenon may be useful for the preparation of proteins.

For Figs. 19 and 20, horse myoglobin (pI = 8.2) and sperm-whale myoglobin (pI = 8.8) was sequentially injected. Sperm-whale myoglobin, the second protein injected, eluted in advance of the first injection.

CONCLUSIONS

Simulations of a chromatographic column were experimentally and computationally performed for the separation of a model mixture of four proteins, sperm-whale myoglobin, horse myoglobin, transferrin, and albumin. A differental model of chromatographic separation with buffering action were proposed, and computer calculations were performed for the simulation of protein separation and focusing effects.

A simulated mixture of the four proteins was eluted at the pH of their isoelectric points, and the internal elution pattern of horse myoglobin was visually determined. The focusing effect of protein by pH was illustrated by the elution of intermittent feeds into a single band.

For smooth and linear pH gradients having interaction with an ion exchanger and mixed buffers, a differential model which included regulation

by buffers was investigated with a model buffer for the pH gradients and the protein elutions. The calculated linear pH gradients and elution profiles showed good agreement with experiments. It was demonstrated that the model is applicable for protein separation and focusing effect. Further, the group dimensionless parameters were introduced to monitor the elution profiles of pH and proteins.

NOMENCLATURE

c	proton concentration in the mobile phase
n	proton concentration in the stationary phase
p_i	protein concentration of compound i in the mobile phase
s_i	protein concentration of compound i in the stationary phase
L	column length (cm)
t	time (minutes)
v	superficial velocity of eluent (cm/min)
D_z	axial dispersion coefficient of proton (cm^2/min)
D_{z_p}	axial dispersion coefficient of protein (cm^2/min)
k_a	adsorption rate constant of proton (1/min)
k_{ad}	adsorption rate constant of protein (1/min)
k_{ad}	adsorption rate coefficient of polyelectrolyte (1/min)
k_d	desorption rate coefficient of polyelectrolyte (concn/min)
K_i	adsorption equilibrium constant of polyelectrolyte, $K_i = k_{ad}/k_d$ (1/concn)
Ke	equilibrium constant (dimensionless)
Ke_p	binding constant of protein
C_e	local equilibrium concentration in the intraparticle space
m	concentration of the solute on the electrolyte
m_t	polyelectrolyte concentration
A, B	characteristic constants in Eq. (31).
C	dimensionless
N	dimensionless
P	dimensionless
S	dimensionless
X	dimensionless length, z/L
Pe	Peclet number for proton (dimensionless), vL/Dz
Pe_p	Peclet number for protein (dimensionless), vL/Dz_p
Pi	dimensionless, $(1 - \epsilon)\epsilon_s/\epsilon$
Po	dimensionless, k_aL/v
Po_p	dimensionless, $k_{ad}L/v$

Greek Symbols

ϵ	void fraction of the bed
ϵ_s	porosity of the particle
τ	dimensionless time, vt/L
θ	fraction of coverage $\theta = K_i C_e/(K_i C_e + 1)$

Subscripts

t	total
z	axial direction
p	protein
i	*i* component

Superscripts

i	input
0	initial equilibrium

REFERENCES

1. Kirk-Othmer, *Encyclopedia of Chemical Technology*, *Vol. 19*, 3rd ed., Wiley, New York, 1981.
2. L. A. Sluyterman, *Philips Tech. Rev.*, *39*(5), 125 (1980).
3. L. A. Osterman, *Methods of Protein and Nucleic Acid Research*, *Vol. 1*, Springer-Verlag, 1984, pp. 155–198.
4. L. A. Sluyterman and O. Elgersma, *J. Chromatogr.*, *150*, 17 (1978).
5. L. A. Sluyterman and J. Wijdenes, *Ibid.*, *150*, 31 (1978).
6. L. A. Sluyterman and J. Wijdenes, *Ibid.*, *206*, 429 (1981).
7. L. A. Sluyterman and J. Wijdenes, *Ibid.*, *206*, 441 (1981).
8. A. T. H. Burness and I. U. Pardoe, *Ibid.*, *259*, 423 (1983).
9. B. Oray, K. U. Yuksel, and R. W. Gray, *Ibid.*, *265*, 126 (1983).
10. N. M. Alexander and W. E. Neeley, *Ibid.*, *230*, 137 (1982).
11. H. J. Marriage and D. J. Harvey, *Ibid.*, *354*, 383 (1986).
12. J. D. Campeau, R. P. Marrs, and G. S. Dizerega, *Ibid.*, *262*, 234 (1983).
13. M. Y. Kamel and S. A. Maksoud, *Ibid.*, *283*, 331 (1984).
14. J. M. Shamoon and I. A. Davies, *Ibid.*, *314*, 499 (1984).
15. R. Scopes, *Protein Purification*, Springer-Verlag, New York, 1982.
16. M. T. W. Hearn and D. J. Lyttle, *J. Chromatogr.*, *218*, 483 (1981).
17. T. W. Hutchens, R. D. Wiehle, N. A. Shahabi, and J. L. Wittliff, *Ibid.*, *266*, 115 (1983).
18. T. W. Hutchens, C. M. Li, and P. K. Besch, *Ibid.*, *359*, 157 (1986).
19. T. W. Hutchens, C. M. Li, and P. K. Besch, *Ibid.*, *359*, 169 (1986).
20. A. Kitahara and A. Watanabe, *Electrical Phenomena at Interfaces*, Dekker, New York, 1984.
21. Y. S. Ghim and H. N. Chang, *Ind. Eng. Chem., Fundam.*, *21*, 369 (1982).
22. Pharmacia Fine Chemicals AB Publications, *Chromatofocusing with Polybuffer and PBE*, Uppsala, Sweden, 1981.
23. T. E. Creighton, *Proteins*, Freeman, New York, 1983.

24. A. Murel, S. Vilde, M. Pank, I. Shevchuk, and O. Kirret, *J. Chromatogr.*, *347*, 325 (1985).
25. A. Murel, S. Vilde, M. Pank, I. Shevchuk, and O. Kirret, *Ibid.*, *362*, 101 (1986).
26. J. Y. Bae, S. W. Chun, and J. D. Kim, *Korean J. Chem. Eng.*, *6*(1), 30 (1989).
27. D. U. Von Rosenberg, *Methods for the Solution of Partial Differential Equations*, Elsevier, New York, 1969.

Received by editor September 6, 1994